

Image Sequence Restoration : A PDE Based Coupled Method for Image Restoration and Motion Segmentation

Pierre Kornprobst^{1,2}, Rachid Deriche¹, and Gilles Aubert²

Pierre.Kornprobst@sophia.inria.fr

<http://www.inria.fr/robotvis/personnel/pkornp/pkornp-eng.html>

¹ INRIA, 2004 route des Lucioles, BP 93, 06902 Sophia-Antipolis Cedex, France

² Laboratoire J.A Dieudonné, UMR n° 6621 du CNRS, 06108 Nice-Cedex 2, France

Abstract. This article deals with the problem of restoring and segmenting noisy image sequences with a static background. Usually, motion segmentation and image restoration are tackled separately in image sequence restoration. Moreover, segmentation is often noise sensitive. In this article, the motion segmentation and the image restoration parts are performed in a coupled way, allowing the motion segmentation part to positively influence the restoration part and vice-versa. This is the key of our approach that allows to deal simultaneously with the problem of restoration and motion segmentation. To this end, we propose a theoretically justified optimization problem that permits to take into account both requirements. A suitable numerical scheme based on half quadratic minimization is then proposed and its stability demonstrated. Experimental results obtained on noisy synthetic data and real images will illustrate the capabilities of this original and promising approach.

1 Introduction

Automatic image sequence restoration is clearly a very important problem. Applications areas include image surveillance, forensic image processing, image compression, digital video broadcasting, digital film restoration, medical image processing, remote sensing . . . See, for example, the recent work done within the European projects, fully or in part, involved with this important problem : *AURORA*, *NOBLESSE*, *LIMELIGHT*, *IMPROOFS*, . . . Image sequence restoration is tightly coupled to motion segmentation. It requires to extract moving objects in order to separately restore the background and each moving region along its particular motion trajectory. Most of the work done to date mainly involves motion compensated temporal filtering techniques with appropriate 2D or 3D Wiener filter for noise suppression, 2D/3D median filtering or more appropriate morphological operators for removing impulsive noise [5, 16, 17, 14, 11, 24, 7, 6]. However, and due to the fact that image sequence restoration is an emerging domain compared to 2D image restoration, the literature is not so abundant than the one related to the problem of restoring just a single image. For example, numerous PDE based algorithms have been recently proposed to tackle the

problems of noise removal, 2D image enhancement and 2D image restoration in real images with a particular emphasis on preserving the grey level discontinuities during the enhancement/restoration process. These methods, which have been proved to be very efficient, are based on evolving nonlinear partial differential equations (PDE's) (See the work of Perona & Malik [27], Nordström, Shah, Osher & Rudin [29], Proesman *et al.* [28], Cottet and Germain, Alvarez *et al* [2], Cohen [8], Weickert [34], Malladi & Sethian [23], Aubert *et al.* [3], You *et al.* [36], Sapiro *et al.* [30], Kornprobst & Deriche [21, 19], . . .).

It is the aim of this article to tackle the important problem of image sequence restoration by applying this PDE based methodology, which has been proved to be very successful in anisotropically restoring images. Therefore, considering the case of an image sequence with some moving objects, we have to consider both motion segmentation and image restoration problems. Usually, these two problems are tackled separately in image sequence restoration. However, it is clear that these two problems must be tackled simultaneously in order to achieve better results. In this article, the motion segmentation and the image restoration parts are done in a coupled way, allowing the motion segmentation part to positively influence the restoration part and vice-versa. This is the key of our approach that allows to deal simultaneously with the problem of restoration and motion segmentation.

The organization of the article is as follows. In Sect. 2, we make some precise recalls about one of our previous approach for denoising a single image [9, 3, 21] The formalism and the methods introduced will be very useful in the sequel. Sect. 3 is then devoted to the presentation of our new approach to deal with the case of noisy images sequence. We formulate the problem into an optimization problem. The model will be clearly explained and theoretically justified in Sect. 3.3. The precise algorithm will be also given and justified. Experimental results obtained on noisy synthetic and real data will then illustrate the capabilities of this new approach in Section 4. We conclude in Sect. 5 by recalling the specificities of that work and giving the future developments.

2 A Variational Method for Image Restoration

In Sect. 2.1, we recall a classical method in image restoration formulated as a minimization problem [9, 4, 3]. Section 2.2 presents a suitable algorithm called the half quadratic minimization.

2.1 A Classical Approach for Image Restoration

Let $N(x, y)$ be a given noisy image defined for $(x, y) \in \Omega$ which corresponds to the domain of the image. We search for the restored image as the solution of the following minimization problem:

$$\inf_I \underbrace{\int_{\Omega} (I - N)^2 d\Omega}_{\text{term 1}} + \alpha^r \underbrace{\int_{\Omega} \phi(|\nabla I|) d\Omega}_{\text{term 2}} \quad (1)$$

where α^r is a constant and ϕ is a function still to be defined. Notice that if $\phi(x) = x^2$, we recognize the *Tikhonov* regularization term. How can we interpret this minimization? In fact, we search for the function I which will be simultaneously close to the initial image N and smooth (since we want the gradient as small as possible). However, this method is well known to smooth the image isotropically without preserving discontinuities in intensity. The reason is that with the quadratic function, gradients are too much penalized. One solution to prevent the destruction of discontinuities but allows for isotropically smoothing uniform areas, is to change the above quadratic term. This point have been widely discussed [31, 32, 4, 3]. We refer to [9] for a review. The key idea is that for low gradients, isotropic smoothing is performed, and for high gradient, smoothing is only applied in the direction of the isophote and not across it. This condition can be mathematically formalized if we look at the Euler-Lagrange Equation (2), associated to energy (1):

$$2(I - N) - \alpha^r \operatorname{div} \left(\frac{\phi'(|\nabla I|)}{|\nabla I|} \nabla I \right) = 0 \tag{2}$$

Let us concentrate on the regularization part associated to the term 2 of (1). If we note $\eta = \frac{\nabla I}{|\nabla I|}$, and ξ the normal vector to η , we can show that:

$$\operatorname{div} \left(\frac{\phi'(|\nabla I|)}{|\nabla I|} \nabla I \right) = \underbrace{\frac{\phi'(|\nabla I|)}{|\nabla I|} I_{\xi\xi}}_{c_\xi} + \underbrace{\phi''(|\nabla I|)}_{c_\eta} I_{\eta\eta} \tag{3}$$

where $I_{\eta\eta}$ (respectively $I_{\xi\xi}$) denotes the second order derivate in the direction η (respectively ξ). If we want a good restoration as described before, we would like to have the following properties:

$$\lim_{|\nabla I| \rightarrow 0} c_\eta = \lim_{|\nabla I| \rightarrow 0} c_\xi = a_0 > 0 \tag{4}$$

$$\lim_{|\nabla I| \rightarrow \infty} c_\eta = 0 \quad \text{and} \quad \lim_{|\nabla I| \rightarrow \infty} c_\xi = a_\infty > 0 \tag{5}$$

If c_ξ and c_η are defined as in (3), it appears that the two conditions of (5) can never be verified simultaneously. So, we will only impose for high gradients [9, 4, 3]:

$$\lim_{|\nabla I| \rightarrow \infty} c_\eta = \lim_{|\nabla I| \rightarrow \infty} c_\xi = 0 \quad \text{and} \quad \lim_{|\nabla I| \rightarrow \infty} \left(\frac{c_\eta}{c_\xi} \right) = 0 \tag{6}$$

Many functions ϕ have been proposed in the literature that comply to the conditions (4) and (6) (see [9]). From now on, ϕ will be a convex function with linear growth at infinity which verify conditions (4) and (6). For instance, a possible choice could be the hypersurface minimal function proposed by Aubert:

$$\phi(x) = \sqrt{1 + x^2} - 1$$

In that case, existence and unicity of problem (1) has recently been shown in the Sobolev space $W^{1,1}(\Omega)$ [4] (See also [33]).

2.2 The Half Quadratic Minimization

The key idea is to introduce a new functional which, although defined over an extended domain, has the same minimum in I as (1) and can be manipulated with linear algebraic methods. The method is based on a theorem inspired from *Geman and Reynolds* [13]. If a function $\phi(\cdot)$ complies with some hypotheses, it can be written in the form:

$$\phi(x) = \inf_d(dx^2 + \psi(d)) \quad (7)$$

where d will be called the dual variable associated to x , and where $\psi(\cdot)$ is a strictly convex and decreasing function. We can verify that the functions ϕ such that (4) (6) are true permit to write (7). Consequently, the problem (1) is now to find I and its dual variable d_I minimizing the functional $\mathcal{F}(I, d_I)$ defined by:

$$\mathcal{F}(I, d_I) = \int_{\Omega} (I - N)^2 d\Omega + \alpha^r \int_{\Omega} d_I |\nabla I|^2 + \psi(d_I) d\Omega \quad (8)$$

It is easy to check that for a fixed I , the functional \mathcal{F} is convex in d_I and for a fixed d_I , it is convex in I . These properties are used to perform the algorithm which consists in minimizing alternatively in I and d_I :

$$I^{n+1} = \operatorname{argmin}_I \mathcal{F}(I, d_I^n) \quad (9)$$

$$d_I^{n+1} = \operatorname{argmin}_{d_I} \mathcal{F}(I^{n+1}, d_I) \quad (10)$$

To perform each minimization, we simply solve the Euler-Lagrange equations, which can be written as:

$$I^{n+1} - N - \alpha^r \operatorname{div}(d_I^n \nabla I^{n+1}) = 0 \quad (11)$$

$$d_I^{n+1} = \frac{\phi'(|\nabla I^{n+1}|)}{|\nabla I^{n+1}|} \quad (12)$$

Notice that (12) gives explicitly d_I^{n+1} while for (11), for a fixed d_I^n , I^{n+1} is the solution of a linear equation. After discretizing in space, we have that $(I_{i,j}^{n+1})_{(i,j) \in \Omega}$ is solution of a linear system which is solved iteratively by the Gauss-Seidel method for example. We refer to [20] for more details about the discretization.

3 The Case of Noisy Images Sequences

Let $N(x, y, t)$ denotes the noisy images sequence for which the background is assumed to be static. A simple moving object detector can be obtained using a thresholding technique over the *inter-frame difference* between a so-called *reference image* and the image being observed. Decisions can be taken independently point by point [10], or over blocks in order to achieve robustness in noise influence [35]. More complex approaches can also be used [26, 1, 15, 22, 5, 16, 17, 14,

11, 24]. However, in our application, we are not just dealing with a motion segmentation problem neither just a restoration problem. In our case, the so-called *reference image* is built at the same time while observing the image sequence. Also, the motion segmentation and the restoration are done in a coupled way, allowing the motion segmentation part to positively influence the restoration part and vice-versa. This is the key of our approach that allows to deal simultaneously with the problem of restoration and motion segmentation.

We first consider that the data is continuous in time. This permit us to present the optimization problem that we want to study (Section 3.1). In Sect. 3.2, we rewrite the problem when the sequence is given only by a finite set of images. This leads to the Problem 2 that will be rigorously justified in Sect. 3.3. The minimization algorithm and its stability are demonstrated in Sect. 3.4.

3.1 An Optimization Problem

Let $N(x, y, t)$ denotes the noisy images sequence for which the background is assumed to be static. Let us describe the unknown functions and what we would like them ideally to be:

- (i) $B(x, y)$, the restored background,
- (ii) $C(x, y, t)$, the sequence which will indicate the moving regions. Typically, we would like that $C(x, y, t) = 0$ if the pixel (x, y) belongs to a moving object at time t , and 1 otherwise.

Our aim is to find a functional depending on $B(x, y)$ and $C(x, y, t)$ so that the minimizers verify previous statements. We propose to solve the following problem:

Problem 1. Let $N(x, y, t)$ given. We search for $B(x, y)$ and $C(x, y, t)$ as the solution of the following minimization problem:

$$\inf_{B,C} \left(\underbrace{\int_t \int_{\Omega} C^2 (B - N)^2 d\Omega dt}_{\text{term 1}} + \alpha_c \underbrace{\int_t \int_{\Omega} (C - 1)^2 d\Omega dt}_{\text{term 2}} + \underbrace{\alpha_b^r \int_{\Omega} \phi_1(|\nabla B|) d\Omega + \alpha_c^r \int_t \int_{\Omega} \phi_2(|\nabla C|) d\Omega dt}_{\text{term 3}} \right) \quad (13)$$

where ϕ_1 and ϕ_2 are convex functions that comply conditions (4) and (6) , and $\alpha_c, \alpha_b^r, \alpha_c^r$ are positive constants.

Getting the minimum of the functional means that we want each term to be small, having in mind the phenomena of the compensations.

The term 3 is a regularization term. Notice that the functions ϕ_1, ϕ_2 have been chosen as in Sect. 2 so that discontinuities may be kept.

If we consider the term 2, this means that we want the function $C(x, y, t)$ to be close to one. In our interpretation, this means that we give a preference to the

background. This is physically correct since the background is visible most of the time. However, if the data $N(x, y, t)$ is too far from the supposed background $B(x, y)$ at time t , then the difference $(B(x, y) - N(x, y, t))^2$ will be high, and to compensate this value, the minimization process will force $C(x, y, t)$ to be zero. Therefore, the function $C(x, y, t)$ can be interpreted as a movement detection function. Moreover, when searching for $B(x, y)$, we will not take into account $N(x, y, t)$ if $C(x, y, t)$ is small (term 1). This exactly means that $B(x, y)$ will be the restored image of the static background.

3.2 The Temporal Discretized Problem

In fact, we have only a finite set of images. Consequently, we are going to rewrite the Problem 1, taking into account that a sequence $S(x, y, t)$ is represented during a finite time by T images noted $S_1(x, y), \dots, S_T(x, y)$. Using these notations for $N(x, y, t)$ and $C(x, y, t)$ permits to rewrite the Problem 1 in the following form:

Problem 2. Let N_1, \dots, N_T be the noisy sequence. We search for B and C_1, \dots, C_T as the solution of the following minimization problem:

$$\inf_{B, C_1, \dots, C_T} \left(\underbrace{\sum_{h=1}^T \int_{\Omega} C_h^2 (B - N_h)^2 d\Omega}_{\text{term 1}} + \alpha_c \underbrace{\sum_{h=1}^T \int_{\Omega} (C_h - 1)^2 d\Omega}_{\text{term 2}} \right. \\ \left. + \underbrace{\alpha_b^r \int_{\Omega} \phi_1(|\nabla B|) d\Omega + \alpha_c^r \sum_{h=1}^T \int_{\Omega} \phi_2(|\nabla C_h|) d\Omega}_{\text{term 3}} \right) \quad (14)$$

This is the problem that we are going to study.

3.3 A Theoretically Justified Method

This section briefly describes the mathematical background of the Problem 2. We will restrict ourself to very general considerations. A complete more theoretical version is now submitted [18]. Notice however that mathematical tools are general and often used in image processing problems.

The proper space to study the Problem 2 is the space of bounded variations, usually noted $BV(\Omega)$ [12]. This space can be considered as a natural extension of the classical Sobolev space $W^{1,1}(\Omega) = \{u \in L^1(\Omega) / \nabla u \in L^1(\Omega)\}$. It can be defined by:

$$BV(\Omega) = \{u \in L^1(\Omega) / Du \in M(\Omega)\}$$

where Du stands for the distributional derivative of u and $M(\Omega)$ the measure space. It is usually used for proving results in image processing since it permits to have jumps along curves which is not possible for functions in $W^{1,1}(\Omega)$. We have the following proposition :

Proposition 1. *The minimization Problem 2, posed over the space $BV(\Omega)^{T+1}$ admits a solution in that space. Moreover it is enough to consider the functions (B, C_1, \dots, C_T) such that:*

$$m_B \leq B \leq M_B \tag{15}$$

$$0 \leq C_h \leq 1 \quad \text{for } h = 1..T \tag{16}$$

$$\text{where } \begin{cases} m_B = \inf_{h \in [0..T], (x,y) \in \Omega} N_h(x, y) \\ M_B = \sup_{h \in [0..T], (x,y) \in \Omega} N_h(x, y) \end{cases} , \tag{17}$$

This remark will be important for the numerical algorithm.

3.4 The Minimization Algorithm

This section is devoted to the numerical study of the Problem 2. If we try to solve directly the Euler-Lagrange equations associated to (14), we will have to cope with non linear equation. To avoid this difficulty, we are going to use the same techniques as developed in the Sect. 2.2. The idea is to introduce dual variables as defined in (7) each time it is necessary. This is the case for the $T + 1$ restoration terms (term 3). Consequently, we introduce the $T + 1$ dual variables noted $d_B, d_{C_1}, \dots, d_{C_T}$ associated respectively to B, C_1, \dots, C_T . Using same arguments as in Sect. 2.2, we will solve, instead of Problem 2, the following problem:

Problem 3. Let N_1, \dots, N_T the noisy sequence. We search for B, d_B, C_1, \dots, C_T and d_{C_1}, \dots, d_{C_T} as the solution of the following minimization problem:

$$\begin{aligned} \inf_{B, C_1, \dots, C_T} & \left(\sum_{h=1}^T \int_{\Omega} [C_h^2 (B - N_h)^2 + \alpha_c (C_h - 1)^2] d\Omega \right. \\ & + \alpha_b \int_{\Omega} [d_B |\nabla B|^2 d\Omega + \Psi_1(d_B)] d\Omega \\ & \left. + \alpha_c \sum_{h=1}^T \int_{\Omega} [d_{C_h} |\nabla C_h|^2 d\Omega + \Psi_2(d_{C_h})] d\Omega \right) \end{aligned} \tag{18}$$

We will note in the sequel $\mathcal{E}(B, d_B, C_h, d_{C_h})$ the corresponding functional. The main observation is that the functional \mathcal{E} is quadratic with respect to B, C_1, \dots, C_T , and convex with respect to d_B and $(d_{C_h})_{h=1..T}$.

Given the initial conditions $(B^0, d_B^0, C_h^0, d_{C_h}^0)$, we iteratively solve the following system :

$$B^{n+1} = \underset{B}{\operatorname{argmin}} \quad \mathcal{E}(B, d_B^n, C_h^n, d_{C_h}^n) \tag{19}$$

$$d_B^{n+1} = \underset{d_B}{\operatorname{argmin}} \quad \mathcal{E}(B^{n+1}, d_B, C_h^n, d_{C_h}^n) \tag{20}$$

$$C_h^{n+1} = \underset{C_h}{\operatorname{argmin}} \quad \mathcal{E}(B^{n+1}, d_B^{n+1}, C_h, d_{C_h}^n) \tag{21}$$

$$d_{C_h}^{n+1} = \underset{d_{C_h}}{\operatorname{argmin}} \quad \mathcal{E}(B^{n+1}, d_B^{n+1}, C_h^{n+1}, d_{C_h}) \tag{22}$$

Equalities (21)-(22) are written for $h = 1..T$. The way to obtain each variable like described in (19)-(22) consists in solving the associated Euler-Lagrange equations. As we are going to see, the dual variables d_B^{n+1} and $(d_{C_h}^{n+1})_{h=1..T}$ are given explicitly, while B^{n+1} and $(C_h^{n+1})_{h=1..T}$ are solutions of linear systems. This linear systems will be solved by an iterative method like Gauss-Seidel's. Equations are:

$$\sum_{h=1}^T C_h^{n2} (B^{n+1} - N_h) - \alpha_b^r \operatorname{div}(d_B^n \nabla B^{n+1}) = 0 \tag{23}$$

$$d_B^{n+1} = \frac{\phi'_1(|\nabla B^{n+1}|)}{|\nabla B^{n+1}|} \tag{24}$$

$$C_h^{n+1} [\alpha_c + (B^{n+1} - N_h)^2] - \alpha_c - 2\alpha_c^r \operatorname{div}(d_{C_h}^n \nabla C_h^{n+1}) = 0 \tag{25}$$

$$d_{C_h}^{n+1} = \frac{\phi'_2(|\nabla C_h^{n+1}|)}{|\nabla C_h^{n+1}|} \tag{26}$$

We next prove that the algorithm described by (23) to (26) is unconditionally stable.

Proposition 2. *Let Ω^d be the set of pixels (i, j) in Ω and let \mathcal{G}^d be the space of functions (B, C_1, \dots, C_T) such that, for all pixels $(i, j) \in \Omega^d$ we have:*

$$m_B \leq B \leq M_B \tag{27}$$

$$0 \leq C_h \leq 1 \quad \text{for } h = 1..T \tag{28}$$

$$0 < m_c \leq \sum_{h=1}^T C_h \leq T \tag{29}$$

$$\text{where } \begin{cases} m_B = \inf_{h=1..T} \inf_{(x,y)} N_h(x, y) \\ M_B = \sup_{h=1..T} \sup_{(x,y)} N_h(x, y) \end{cases}, \quad m_c = \frac{T\alpha_c^r}{\alpha_c + (M_B - m_B)^2 + 4} \tag{30}$$

Then, for a given $(B^n, C_1^n, \dots, C_T^n)$ in \mathcal{G}^d , there exists a unique $(B^{n+1}, C_1^{n+1}, \dots, C_T^{n+1})$ in \mathcal{G}^d such that (23)-(26) are satisfied.

The proof is based on the application of the fixed point theorem. We refer to [20] for more details. Anyway, let us remark that the boundaries (27) and (28)

can be justified if we consider the continuous case (see (17)). As for condition (29), it is also very natural if we admit the interpretations of the variables C_h : if this condition is false, this would mean that the background is never seen at some points which we refuse.

To conclude this section, we will notice that if $\alpha_c^r = 0$, the functions $(C_h^{n+1})_{h=1..T}$ are in fact obtained explicitly by:

$$C_h^{n+1} = \frac{\alpha_c}{\alpha_c + (B^{n+1} - N_h)^2} \quad (31)$$

As we can imagine, this case permits important reduction of the computational cost since T linear systems are replaced by T explicit expressions. We will discuss in Sect. 4 if it is worth regularizing or not the functions C_h .

4 The Numerical Study

This section aims at showing quantitative and qualitative results about this method. Synthetics noisy sequences will be used to estimate rigorously the capabilities of our approach. The purpose of Sect. 4.1 is the quality of the restoration. The Sect. 4.2 is devoted to the movement detection and its sensibility with respect to noise. We will conclude in Sect. 4.3 by real sequences.

4.1 About the Restoration

To estimate the quality of the restoration, we used the noisy synthetic sequence presented in Fig. 1 (a)(b). Figure 1 (c) is a representation of the noisy background without the moving objects. We mentioned the value of the Signal to Noise Ratio (SNR) usually used in image restoration to quantify the results quality. We refer to [21] for more details. We recall that the higher the SNR is, the best the quality is. Usually used to extract the foreground from the background, the median (see Fig. 1 (d)) appears to be inefficient. The average in time of the sequence (see Fig 1 (e)), although it permits a noise reduction, keeps the trace of the moving objects. The Fig. 1 (f) is the result that we obtained.

To conclude that section, let us mention that we also tried the case $\alpha_c^r = 0$, that is to say we did not regularized the functions C_h . The resulting SNR was 14, to be compared with 14.4 ($\alpha_c^r \neq 0$). This leads to the conclusion that regularizing the functions C_h is not very important. However, this point has to be better investigated and more experimental results have to be considered before to conclude.

4.2 The Sensitivity of Object Detection With Respect to Noise

In this section, we aim at showing the robustness of our method with respect to noise. To this end, we choose a synthetic sequence where an object (denoted \odot) is translating on a uniform black background (See Fig. 2). Both kind of noise have been experimented : Gaussian and uniform. The Gaussian noise is

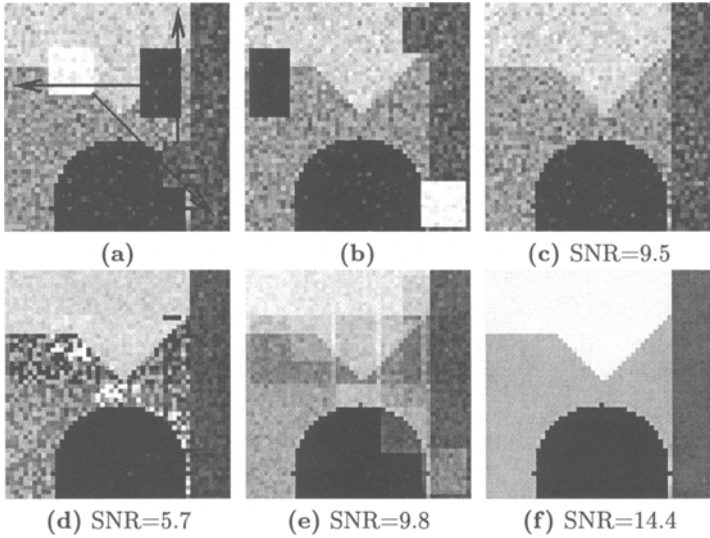


Fig. 1. Results on a synthetic sequence (5 images) (a) Description of the sequence (first image) (b) Last image of the sequence (c) The noisy background without any objects (d) Mediane (e) Average (f) Restored background ($\alpha_c^\epsilon \neq 0$)



Fig. 2. The original synthetic sequence used for tests. A white object (noted \odot) is translating from left to right. 35 images are available.

| Gaussian Noise | | | | |
|----------------|-------------------|-------------|---------|-----------|
| σ | $\text{SNR}(N_h)$ | $\sigma(B)$ | \odot | \square |
| 0 | 0 | 0 | 0 | 0 |
| 5 | 14.7 | 0.9 | 0 | 0 |
| 10 | 9.2 | 1.8 | 0 | 0 |
| 15 | 6.2 | 3.0 | 0.1 | 0 |
| 20 | 4.5 | 4.5 | 1.5 | 0.7 |
| 25 | 3.3 | 6.3 | 4.9 | 3.2 |
| 30 | 2.4 | 8.4 | 9.5 | 7.6 |

| Uniform Noise | | | | |
|---------------|-------------------|-------------|---------|-----------|
| % | $\text{SNR}(N_h)$ | $\sigma(B)$ | \odot | \square |
| 0 | 0 | 0 | 0 | 0 |
| 5 | 6.8 | 0.3 | 2.9 | 2.2 |
| 10 | 4.3 | 0.4 | 5.5 | 4.5 |
| 15 | 3.3 | 0.6 | 8.5 | 6.7 |
| 20 | 2.3 | 0.7 | 11.0 | 8.6 |
| 25 | 2.0 | 1.5 | 14.1 | 10.8 |

Table 1. Quantitative measures for tests about robustness to noise (Gaussian and uniform). $\text{SNR}(N_h)$ =signal to noise ratio for one image of the data. $\sigma(B)$ =root of the variance of the restored background \odot =percentage of bad detections for the moving object \square =percentage of bad detections for the background. See also Fig. 3 for two examples for equivalent noises.

characterized by its variance σ (the average equals to zero), while the uniform noise is defined by a percentage of modified pixels. We recall that a uniform noise of $X\%$ means that $X\%$ of pixels will be replaced by a value between the minimum and the maximum value of the image with a uniform distribution. Results are reported in Tab. 1 and Fig. 3. Notice that we also wrote the root of the variance of the restored background B which is a good indicator here for estimating the accuracy, since the ideal image is a constant image.

The criterion used to decide whether a pixel belongs to the background or not is : if $C_h(i, j) > \text{threshold}$, then the pixel (i, j) of the image number h belongs to the background. Otherwise, it belongs to a moving object. The threshold has been fixed to 0.25 in all experiments.

Finally, notice that same parameters ($\alpha_b^t, \alpha_c, \alpha_c^t$) have been used for all experiments. Generally speaking, we remarked that the algorithm performs well on a wide variety of sequences with the same set of parameters.

4.3 Some Real Sequences

The first real sequence is presented in Fig. 4 (a). A small noise is introduced by the camera and certainly by the hard weather conditions. Notice the reflections on the ground which is frozen. We show in Fig. 4 (b) the average in time of the sequence. The restored background is shown in Fig. 4 (c). As we can see, it has been very well found and enhanced. Figure 4 (d) is a representation of the function C_h where moving regions have been replaced by the original intensities.

The second sequence is more noisy than the first one. Its description is given in Fig. 5 (a). To evaluate the quality of the restoration, we show a close-up of the same region for one original image (see Fig. 5 (b)), the average in time (see Fig. 5 (c)) and the restored background B (see Fig. 5 (d)). The detection of moving regions is displayed in Fig. 5 (e). Notice that some sparse motion have been detected at the right bottom and to left of the two persons. They correspond to the motion of a bush and the shadow of a tree due to the wind.

5 Conclusion

We have presented in this article an original coupled method for the problem of image sequence restoration and motion segmentation. This original way to restore image sequence has been proved to give very promising result. To complete this work, several ideas are considered : use the motion segmentation part to restore also the moving regions, think about possible extensions for non-static cameras. This is the object of our current work.

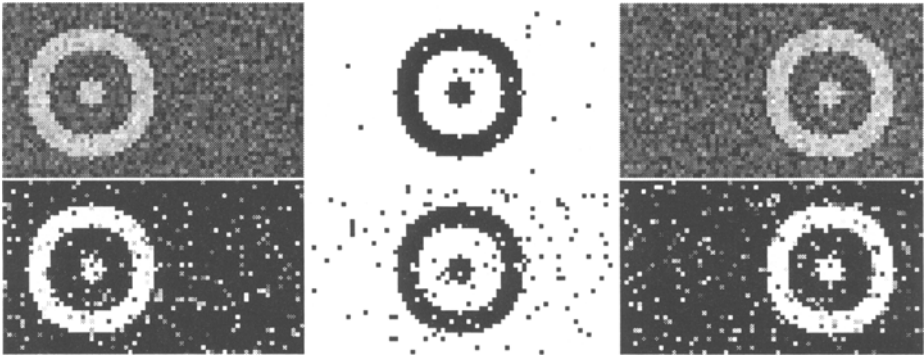


Fig. 3. Results about noise robustness. First row : gaussian noise of variance 20. Second row : uniform noise of percentage 10. Left and Right : images from the sequence. Middle : function C_h .

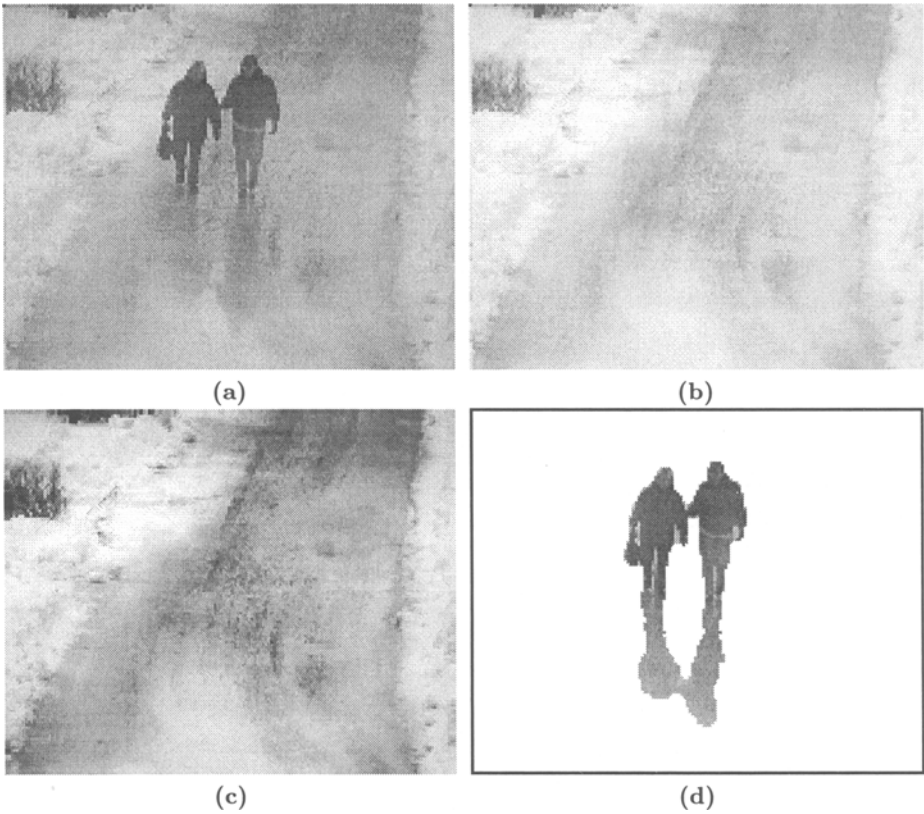


Fig. 4. (a) Description of the sequence (55 images available). Two people are walking from top to bottom (b) The average over the time (c) The restored background B (d) Using function C_h , we replaced moving regions by the data intensity.

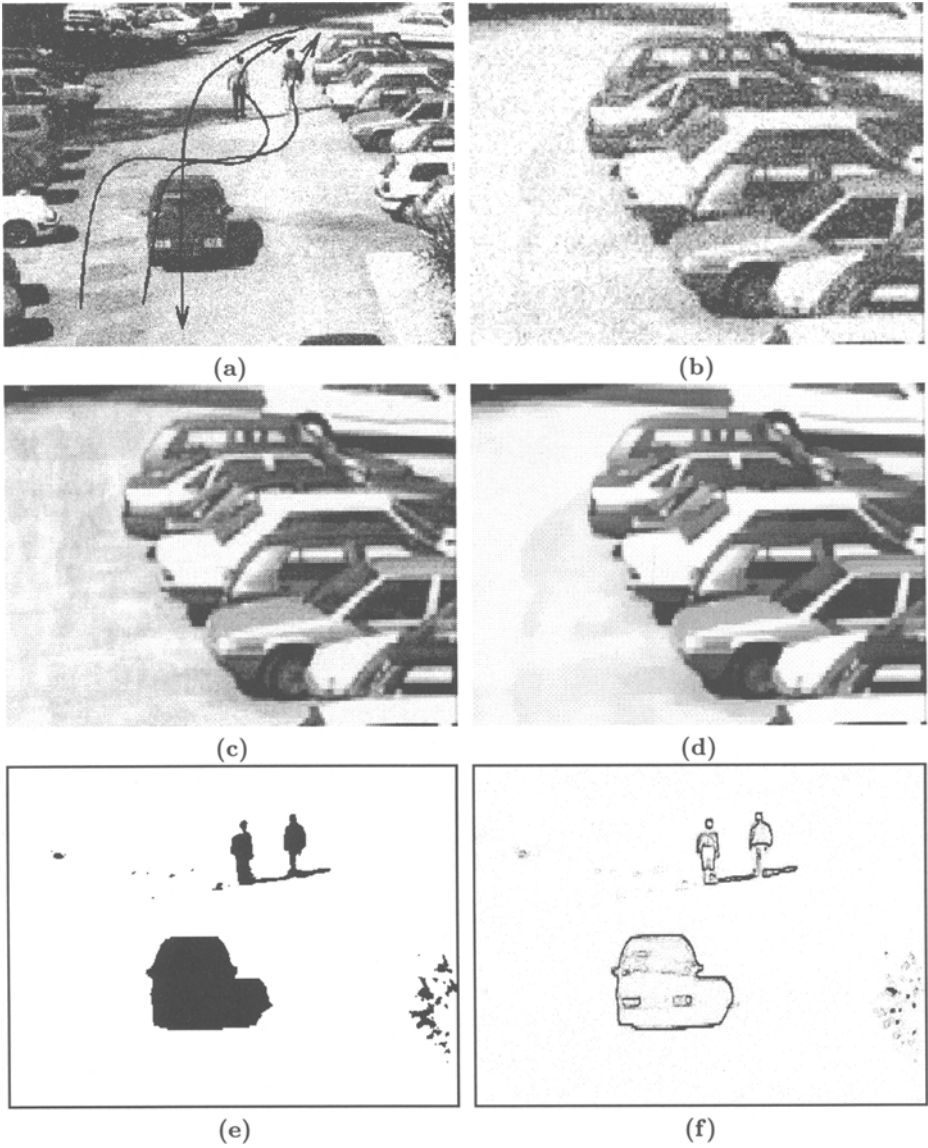


Fig. 5. (a) Description of the sequence (12 images available) (b) Zoom on a upper right part of the original sequence (without objects) (c) Zoom on the mean image (d) Zoom on the restored background B (e) The function C_h thresholded (f) The dual variable d_{ch} .

References

1. T. Aach and A. Kaup. Bayesian algorithms for adaptive change detection in image sequences using markov random fields. *Signal Processing: Image Communication*, 7:147–160, 1995.
2. L. Alvarez and L. Mazorra. Signal and image restoration using shock filters and anisotropic diffusion. *SIAM Journal of numerical analysis*, 31(2):590–605, Apr. 1994.
3. G. Aubert, M. Barlaud, L. Blanc-Feraud, and P. Charbonnier. Deterministic edge-preserving regularization in computed imaging. *IEEE Trans. Imag. Process.*, 5(12), Feb. 1997.
4. G. Aubert and L. Vese. A variational method in image recovery. *SIAM J. Numer. Anal.*, 34(5):1948–1979, Oct. 1997.
5. J. Boyce. Noise reduction of image sequences using adaptative motion compensated frame averaging. In *IEEE ICASSP*, volume 3, pages 461–464, 1992.
6. J. Brailean and A. Katsaggelos. Simultaneous recursive displacement estimation and restoration of noisy-blurred image sequences. *IEEE Transactions on Image Processing*, 4(9):1236–1251, Sept. 1995.
7. O. Buisson, B. Besserer, S. Boukir, and F. Helt. Deterioration detection for digital film restoration. In *Computer Vision and Pattern Recognition*, pages 78–84, Puerto Rico, June 1997.
8. L. D. Cohen. Auxiliary variables and two-step iterative algorithms in computer vision problems. *ICCV*, 1995.
9. R. Deriche and O. Faugeras. Les EDP en traitement des images et vision par ordinateur. Technical report, INRIA, Nov. 1995. A more complete version of this Research Report has appeared in the French Revue "Traitement du Signal". Volume 13 - No 6 - Special 1996.
10. N. Diehl. Object-oriented motion estimation and segmentation in image sequences. *IEEE Transactions on Image Processing*, 3:1901–1904, Feb. 1990.
11. E. Dubois and S. Sabri. Noise reduction in image sequences using motion-compensated temporal filtering. *IEEE Transactions on Communications*, 32(7):826–831, July 1984.
12. L. C. Evans and R. F. Garipey. *Measure Theory and Fine Properties of Functions*. CRC, 1992.
13. D. Geman and G. Reynolds. Constrained restoration and the recovery of discontinuities. *IEEE Transactions on Pattern Analysis and Machine Intelligence*, 14(3):367–383, 1993.
14. S. Geman, D. E. McClure, and D. Geman. A nonlinear filter for film restoration and other problems in image processing. *CVGIP : Graphical Models and Image Processing*, 54(4):281–289, July 1992.
15. K. Karmann, A. Brandt, and R. Gerl. Moving object segmentation based on adaptive reference images. *Signal Processing: Theories and Applications*, V:951–954, 1990.
16. A. Kokaram. Reconstruction of severely degraded image sequences. In *International Conference on Image Applications and Processing*, Florence, Italy, 1997.
17. A. C. Kokaram and S. Godsill. A system for reconstruction of missing data in image sequences using sampled 3d ar models and mrf motion priors. In B. Buxton, editor, *Proceedings of the 4th European Conference on Computer Vision*, pages 613–624, Cambridge, UK, Apr. 1996.

18. P. Kornprobst, G. Aubert, and R. Deriche. A variational method for image sequences interpretation (submitted). 1997.
19. P. Kornprobst, R. Deriche, and G. Aubert. Image coupling, restoration and enhancement via PDE's. In *International Conference on Image Processing*, volume II of III, pages 458–461, Santa-Barbara, California, Oct. 1997.
20. P. Kornprobst, R. Deriche, and G. Aubert. Image Sequence Restoration : A PDE Based Coupled Method for Image Restoration and Motion Segmentation. Technical Report 3308, INRIA, Nov. 1997.
21. P. Kornprobst, R. Deriche, and G. Aubert. Nonlinear operators in image restoration. In *Proceedings of the International Conference on Computer Vision and Pattern Recognition*, pages 325–331, Puerto-Rico, June 1997. IEEE.
22. S. Liou and R. Jain. Motion detection in spatio-temporal space. *Computer Vision, Graphics and Image Understanding*, (45):227–250, 1989.
23. R. Malladi and J. Sethian. Image processing: Flows under min/max curvature and mean curvature. *Graphical Models and Image Processing*, 58(2):127–141, Mar. 1996.
24. R. Morris. *Image Sequence Restoration using Gibbs Distributions*. PhD thesis, Cambridge University, England, 1995.
25. N. Paragios and R. Deriche. A PDE-based Level Set Approach for Detection and Tracking of Moving Objects. In *Proceedings of the 6th International Conference on Computer Vision*, Bombay, India, Jan. 1998. IEEE Computer Society Press.
26. N. Paragios and G. Tziritas. Detection and localization of moving objects in image sequences. *FORT-Hellas Technical Report, Accepted for publication in Signal Processing: Image Communication*, Oct. 1996.
27. P. Perona and J. Malik. Scale-space and edge detection using anisotropic diffusion. *IEEE Transactions on Pattern Analysis and Machine Intelligence*, 12(7):629–639, July 1990.
28. M. Proesmans, E. Pauwels, and L. V. Gool. *Coupled Geometry-Driven Diffusion Equations for Low-Level Vision*, pages 191–228. Computational imaging and vision. Kluwer Academic Publishers, 1994.
29. L. Rudin and S. Osher. Total variation based image restoration with free local constraints. In *International Conference on Image Processing*, volume I, pages 31–35, Nov. 1994.
30. G. Sapiro, A. Tannenbaum, Y. You, and M. Kaveh. Experiments on geometric image enhancement. In *International Conference on Image Processing*, 1994.
31. C. Schnörr. Unique reconstruction of piecewise-smooth images by minimizing strictly convex nonquadratic functionals. *Journal of Mathematical Imaging and Vision*, 4:189–198, 1994.
32. R. Stevenson, B. Schmitz, and E. Delp. Discontinuity preserving regularization of inverse visual problems. *IEEE Transactions on Systems, Man, and Cybernetics*, 24(3):455–469, Mar. 1994.
33. L. Vese. *Problèmes variationnels et EDP pour l'analyse d'images et l'évolution de courbes*. PhD thesis, Université de Nice Sophia-Antipolis, Nov. 1996.
34. J. Weickert. *Anisotropic Diffusion in Image Processing*. PhD thesis, University of Kaiserslautern, Germany, Laboratory of Technomathematics, Jan. 1996.
35. O. Wenstop. Motion detection from image information. *Proceedings in Scandianvian Conference on Image Analysis*, pages 381–386, 1983.
36. Y. You, M. Kaveh, W. Xu, and A. Tannenbaum. Analysis and Design of Anisotropic Diffusion for Image Processing. In *International Conference on Image Processing*, volume II, pages 497–501, Nov. 1994.